Received: 19 September 2023 | Revised: 24 January 2024 | Accepted: 12 February 2024

DOI: 10.1111/cas.16122

ORIGINAL ARTICLE

Cancer Science WILEY

# RB1 loss induces quiescent state through downregulation of RAS signaling in mammary epithelial cells

Linxiang Gong[1] | Dominic Chih-Cheng Voon[2] | Joji Nakayama[1] | Chiaki Takahashi[1] | Susumu Kohno[1]

[1]Division of Oncology and Molecular Biology, Cancer Research Institute, Kanazawa University, Kanazawa, Ishikawa, Japan

[2]Institute for Frontier Science Initiative, Kanazawa University, Kanazawa, Ishikawa, Japan

**Correspondence**
Susumu Kohno and Chiaki Takahashi, Division of Oncology and Molecular Biology, Cancer Research Institute, Kanazawa University, Kanazawa, Ishikawa, Japan.
Email: skohno@staff.kanazawa-u.ac.jp and chtakaha@staff.kanazawa-u.ac.jp

**Funding information**
Japan Agency for Medical Research and Development, Grant/Award Number: 19cm0106164h0001; Japan Society for the Promotion of Science, Grant/Award Number: 17H03576, 17K14992, 17K19586, 19K22555, 20K07612, 22K07209 and 23KJ1033; Daiichi-Sankyo, Grant/Award Number: TaNeDS (C1010568); Japan Science and Technology Corporation, Grant/Award Number: Next Generation World-Leading Researchers (LS049)

## Abstract

While loss of function (LOF) of retinoblastoma 1 (RB1) tumor suppressor is known to drive initiation of small-cell lung cancer and retinoblastoma, RB1 mutation is rarely observed in breast cancers at their initiation. In this study, we investigated the impact on untransformed mammary epithelial cells given by RB1 LOF. Depletion of RB1 in anontumorigenic MCF10A cells induced reversible growth arrest (quiescence) featured by downregulation of multiple cyclins and MYC, upregulation of $p27^{KIP1}$, and lack of expression of markers which indicate cellular senescence or epithelial–mesenchymal transition (EMT). We observed a similar phenomenon in human mammary epithelial cells (HMEC) as well. Additionally, we found that RB1 depletion attenuated the activity of RAS and the downstream MAPK pathway in an RBL2/p130-dependent manner. The expression of farnesyltransferase β, which is essential for RAS maturation, was found to be downregulated following RB1 depletion also in an RBL2/p130-dependent manner. These findings unveiled an unexpected mechanism whereby normal mammary epithelial cells resist to tumor initiation upon RB1 LOF.

**KEYWORDS**
MYC, quiescence, RAS, RB1, RBL2/p130

## 1 | INTRODUCTION

The RB1 tumor suppressor gene product lacks enzymatic activity yet plays a crucial role in transcriptional regulation by interacting with executive molecules, including various chromatin modifiers and tissue-specific transcription factors. RB1 binds to three members of the E2F family of transcription factors and represses their activity, which results in the downregulation of a number of genes required for cell cycle progression.[1] RB1 mutation or deletion contributes to the initiation of limited types of cancer, including small-cell lung cancer and retinoblastoma. In the majority of cancer types, RB1 LOF takes place mostly during their malignant progression.[2] There might be a mechanism whereby RB1 LOF does not initiate malignant transformation in tissues that generate the latter type of

**Abbreviations:** CDK, cyclin-dependent kinases; CDT1, chromatin licensing and DNA replication factor 1; DOX, doxycycline; EMT, epithelial–mesenchymal transition; FTβ, farnesyltransferase β; HMEC, human mammary epithelial cells; LOF, loss of function; MOSE, mouse ovary surface epithelium cells; RB1, retinoblastoma 1; RBD, RAS-binding domain; RBL2, retinoblastoma-like protein 2; SA-β-gal, senescence-associated β-galactosidase.

tumors. RB1 LOF in mouse C cells activates Ras through enhanced isoprenylation, leading to oncogene-induced senescence via DNA damage-mediated induction of $p16^{Ink4A}$, preventing C cells from progressing to adenocarcinoma from adenoma. However, simultaneous loss of Ink4A or N-ras in Rb1-deficient C cell tumor cells was found to prevent cellular senescence and allow C cell adenoma to progress to adenocarcinoma.[3] The ectopic expression of oncogenic RAS in fibroblasts causes cellular senescence due to replication stress and subsequent DNA damage. This process is counteracted by RB1.[4] These reports suggest that the activation of RAS may antagonize RB1 LOF-induced carcinogenesis.

Dormancy is a cellular state where cells exit the cell cycle and remain undivided for prolonged periods yet retaining the ability to re-enter the cell cycle. In most cases, quiescent cells arrest at the G0 phase, a phase distinct from the G1 or S phase.[5] Cyclin D-CDK4/6 and cyclin E-CDK2 complexes drive cell cycle progression. The expression of these protein complexes is typically suppressed in quiescent cells, resulting in RB1 being under-dephosphorylated. In addition, RAS signaling causes the destabilization and mislocalization of a CDK inhibitor $p27^{KIP1}$ through phosphorylation at serine 10.[6] Inhibition of CDK4/6 activity by the synthetic CDK4/6 inhibitor palbociclib elicits cell cycle stasis in cancer cells that are RB1 intact.[7] Conversely, in certain contexts, $p27^{KIP1}$ is known to interact with active CDK4 and cyclin D1, subsequently becoming insensitive to palbociclib.[8] S-phase kinase-associated protein 2 (Skp2) facilitates the degradation of $p27^{KIP1}$ via ubiquitination. RB1 modulates Skp2 activity by interacting with Skp2's substrate-binding site, leading to the induction of cell cycle arrest in cancer cells. Overall, RAS signaling counters carcinogenesis or malignant transformation through INK4A, while RB1 LOF-induced RAS activation promotes the loss of cell cycle control via $p27^{KIP1}$ inactivation. However, it remains unclear whether the loss of RB1 can promote initial transformation in noncarcinogenic cells lacking INK4A.

In this study, we observed a quiescent state in MCF10A cells following RB1 depletion. MCF10A is a non-neoplastic human mammary epithelial cell line with intact TP53 and a focal deletion of INK4A. Upon characterization of RB1-depleted MCF10A cells, we found attenuation in cellular proliferation and growth signaling, indicating the importance of RB1 in maintaining normal cell growth. Our results may clarify the mechanism whereby carcinogenesis induced by RB1 deficiency is counteracted in normal cellular context.

## 2 | MATERIALS AND METHODS

### 2.1 | Cell culture

MCF10A cells were purchased from ATCC, and Human Mammary Epithelial Cells (HMEC) were purchased from Thermo Fisher Scientific (A10565). These cells were cultured in mammary epithelium basal medium (MEBM, #CC-4136, Lonza) supplemented with bovine pituitary extract (#CC-4009G, Lonza), 20 ng/mL hEGF (#CC-4017G, Lonza), 10 μg/mL insulin (#CC-4021G, Lonza), 0.5 mg/mL hydrocortisone (#CC-4031G, Lonza), and 100 ng/mL cholera toxin solution (#030–20621, Wako). HEK293T (#RCB2002) and MIA-PACA-2 (#RCB2094) were purchased from RIKEN BRC. p53-deficient mouse ovary surface epithelium (MOSE) cells (#JCRB0151.1) were purchased from JCRB cell bank and cultured in Dulbecco's modified Eagle's medium (#04129775, Wako) supplemented with 10% fetal bovine serum (FBS, #10270-106, Thermo Fisher Scientific) and 1% penicillin–streptomycin solution (#16823291, Wako). All cells were maintained in a humidified $CO_2$ incubator at 37°C. Mycoplasma infection was regularly checked by PCR using the following sequences of the primers: forward: ACACCATGGGAGCTGGTAAT, reverse: CTTCWATCGACTTYCAGACCCAAGGC.

### 2.2 | Generation of lentivirus

MISSION TRC human RB1 shRNA (TRCN0000040163 and TRCN0000010419), mouse Rb1 shRNA (TRCN0000042543 and TRCN0000042544), and negative control (Scramble, SHC002) were purchased from Merck. c-Myc overexpression plasmid was purchased from Addgene (#20723), and CS-IV TRE-RfA-UbC-Puro-H-$RAS^{G12V}$ was a kind gift from Yoshikazu Johmura. For CRISPR gRNA, the following sequences were used: human RB1 gRNA: TAGGCTAGCCGATACACTGT, human RBL2 gRNA: CTCTCAAGGTGTCTGAACGC. For handling lentivirus, we strictly followed the National Institutes of Health guidelines. To generate lentivirus, $4 \times 10^6$ HEK293T cells were seeded onto a D100 dish and transfected with 5 μg of targeting vector, mixed with 0.5 μg of pCMV-VSVG and 4.5 μg of packaging vector PAX2, and with 27 μg polyethyleneimine (#24765, Polysciences, Inc) overnight and replaced with fresh culture media. The media containing lentivirus were collected after 48 h of transfection, then passed through a 0.45-μm filter, and concentrated with polyethylene glycol.

### 2.3 | Lentivirus infection

A total of $0.5 \times 10^5$ cells were seeded onto 12-well plates and cultured. After overnight culture, the medium was replaced with fresh media containing lentivirus and 1 μg/mL polybrene. After overnight infection, cells were subjected to selection with 1 μg/ml puromycin (#ant-pr-1, Invivogen) for 72 h. For H-RAS induction, cells were subjected to selection with 200 μg/mL hygromycin for 72 h.

### 2.4 | Immunoblotting

A total of $1.5 \times 10^5$ cells were seeded onto six-well plates and cultured overnight. After treatment, cells were harvested using magnesium-containing lysis buffer (MLB) supplemented with 0.5 mM NaF, 100 μM $Na_3VO_4$, and 1x protease inhibitor (#25955-11, Nacalai Tesque). Immunoblotting was performed as previously described.[9] Antibodies are listed in Table S1.

### 2.5 | Immunocytochemistry

A total of 0.3 $\times 10^5$ cells were seeded onto the coverslips coated with poly-L-lysine solution (#RNBK1397, Sigma) in six-well plates. After transduction of shRNA for 3 days, cells were fixed with 4%-paraformaldehyde (4% PFA, #09154-85, Nacalai Tesque) at room temperature (RT) for 10 min and permeabilized using 0.5% Triton X-100 (#12967-45, Nacalai Tesque) at RT for 5 min. Then, cells were blocked with 5% BSA at RT for 1 h and incubated with primary antibody at 4°C overnight. After incubation, cells were washed with phosphate-buffered saline-tween 20 (PBS-T) and incubated with a secondary antibody at RT for 1 h in the dark and mounted with DAPI (#ZF0826, VECTASHIELD). Antibodies are listed in Table S1. Fluorescent images were captured on KEYENCE BZ-9000.

### 2.6 | Flow cytometry

After induction of gRNA for RB1 and selection with puromycin, MCF10A cells were dissociated using Accutase Cell Detachment Solution (#30051580, Innovative Cell Technologies). Then, cells were fixed with 4%PFA at RT for 10 min and were permeabilized with 0.5% Triton X-100 at RT for 5 min. Afterward, cells were blocked with 5% BSA at RT for 1 h and incubated with Ki67 antibody at 4°C overnight. After incubation, cells were washed with PBS-T and incubated with a secondary antibody at RT for 1 h in the dark. Cells were analyzed by FACSCanto Flow Cytometer.

### 2.7 | Colony formation

A total of 3 $\times 10^3$ cells were seeded onto a D60 dish and cultured for 10 days. Cells were washed with PBS and were fixed with 4% PFA at RT for 10 min. Then, cells were washed with PBS and stained with 0.5% crystal violet solution (#031-04852, Wako) for 30 min. After staining, cells were washed with tap water. The number of colonies was quantified by Image J.

### 2.8 | Ras-GTP assay

The pull-down assay to measure RAS activity was performed following previously established protocols.[3] Briefly, the cells were lysed in MLB in the presence of a protease inhibitor mixture. The lysates were clarified by centrifugation, and the protein concentration was determined using a BCA assay. Subsequently, 300 μg of cell protein was incubated with the recombinant RAS-binding domain (RBD) of Raf1-149 fused to glutathione-S-transferases (GST-RBD). The active Ras complex was precipitated using glutathione-conjugated agarose beads (#17-0756-01, Merck). After overnight incubation at 4°C, the beads were washed with buffer, suspended in 15 μL of SDS-PAGE sample buffer, and loaded onto a 16% SDS-PAGE gel for immunoblotting.

### 2.9 | Sphere assay

Cells were pretreated with 1 μg/mL doxycycline (DOX) for 24 h. Then 50,000 cells were seeded onto a six-well plate (#4810-800LP, AGC), with 1x αMEM medium (#1031126, MP Biomedicals) containing 1% methylcellulose (#138–05052, Wako), B27 (#17504-044, Thermo Fisher Scientific), 100 μg/mL EGF, 100 μg/mL bFGF, 10 μg/mL insulin, with or without 1 μg/mL DOX for 14 days. Images were captured and quantified by KEYENCE BZ-9000.

### 2.10 | SA-β-gel staining

SA-β-gel staining to detect senescence cells was performed as previously described.[7]

### 2.11 | RT-PCR

Total RNA was isolated from MCF10A cells using TRIzol (#15596018, Thermo Fisher Scientific) according to the manufacturer's instructions. Quantitative RT-PCR of total RNA was carried out using a high-capacity RNA-to-cDNA kit (#4387406, Thermo Fisher Scientific) and EagleTaq master mix with ROX (#05876486001, Roche) using LightCycler 480 System (Roche) according to the manufacturer's instruction.

TaqMan probes and primers used were as follows: CDH1 (Hs01023894_m1), TWIST1 (Hs01675818_s1), SNAI1 (Hs00195591_m1), ZEB1 (Hs00232783_m1), MYC (forward: AATGAAAAGGCCCCCAAGGTAGTTATCC, reverse: GTCGTTTCCGCAACAAGTCCTCTTC). The relative level of gene expression was normalized using the level of TBP (Hs00427620_m1) or RPLP0 (forward: GTCCTCGTGGAAGGCCC, reverse: AGGAGAGACAGGGAGCTCAG). The values represent the average of three biological replicates.

### 2.12 | Statistical analysis

Statistical significance was calculated by using Student's *t*-test or ANOVA followed by post hoc Tukey's test for more than three groups. *p*-Values less than 0.05 were considered statistically significant. $^*p<0.05$, $^{**}p<0.01$, $^{***}p<0.001$, $^{****}p<0.0001$, ns not significant.

## 3 | RESULTS

### 3.1 | RB1 loss induces growth arrest in mammary epithelial cells

To investigate the impact of RB1 depletion on breast cancer initiation, we employed lentiviral-mediated short hairpin RNA technology to deplete RB1 in a nontumorigenic mammary epithelial

cell line MCF10A. MCF10A cells exhibited typical epithelial morphology characterized by a round shape and distinct epithelial clusters. After 72 h of transduction, RB1-depleted cells exhibited a fibroblast-like morphology (Figure 1A). The E-cadherin–β-catenin complex specifically localizes to the cell membrane and plays a crucial role in maintaining epithelial integrity. In MCF10A cells, β-catenin localized to the plasma membrane, while RB1 depletion caused β-catenin translocation from the cell membrane to the cytosolic compartment (Figure S1). Transforming growth factor-β (TGF-β) initiates epithelial–mesenchymal transition (EMT) in various epithelial cell lines, including MCF10A and MDCK cells. EMT occurs by the upregulation of EMT-associated genes such as ZEB1, TWIST, and SNAI1.[10] Translocation of β-catenin from cellular membrane occurs in response to TGF-β stimulation. In addition, MCF10A cells expressing ZEB1 by the treatment with TGF-β exhibit decreased entry into S phase in MCF10A cells.[11,12] In RB1-deficient MCF10A cells, we observed a significant reduction in colony number and proliferation (Figure 1B). Despite the presence of β-catenin translocation to the cytoplasmic compartment, we did not detect any significant alterations in the expression of epithelial and EMT markers (Figures S2 and S3). Further analysis revealed that RB1 deficiency in MCF10A cells led to a significant reduction in the protein levels of cyclins A, B1, D1, E, geminin, and CDT1 and upregulation of $p27^{KIP1}$, when compared with control cells (Figure 1E). Similar phenotypes were also discerned in HMEC but not in Trp53-deficient MOSE cells (Figure S4A,B). Quiescence is characterized by reversible proliferative arrest, in which cells remain inactive but retain the ability to re-enter the cell cycle upon receiving appropriate stimulation. One of the primary mechanisms for cells to enter a quiescent state is the suppression of Ki67 expression and induction of cyclin inhibitors.[5] Furthermore, depletion of RB1 in MCF10A led to a decreased ratio of Ki67-positive cells (Figure 1F,G). These data suggest that RB loss in MCF10A cells induces quiescent state.

In a previous study, we reported that Rb1 loss in mouse thyroid caused calcitonin-producing (C) cell-derived adenoma. The presence of N-ras prevents adenoma from progressing to adenocarcinoma due to senescence triggered by augmented $p16^{Ink4A}$ expression via DNA damage response caused by enhanced N-RAS activation.[3] MCF10A cells have a hemizygous deletion of the INK4A locus but retain the intact p53-$p21^{WAF1/CIP1}$ pathway.[13,14] To assess the cellular senescence in growth-arrested cells, we conducted senescence-associated β-galactosidase (SA-β-gal) staining and immunoblotting for p53 and $p21^{WAF1/CIP1}$ in RB1-depleted MCF10A cells. We did not detect SA-β-gal-positive cells in either the control or RB depletion, nor increases in p53 or $p21^{WAF1/CIP1}$ (Figures S5 and S6). To determine if there has been an increase in DNA damage upon RB1 knockdown, we measured γ-H2AX levels in cells to estimate a degree of DNA damage using immunoblotting and immunocytochemistry but found no increase (Figures S5 and S7). These data suggest that the cell cycle arrest caused by RB1 loss in MCF10A cells takes place without exhibiting the features of cellular senescence or DNA damage response.

### 3.2 | RB1 loss induces c-Myc degradation

The upregulation of D-type cyclins is crucial in response to mitogenic signals. It plays a pivotal role in facilitating cell cycle progression through the G1-S transition by triggering the phosphorylation of RB1 by CDK4/6 and CDK2.[15] We observed a reduction in Ki67-positive cells and a decrease in the expression of cyclin D1 and E in RB1-depleted MCF10A cells (Figure 1E–G). We then investigated the mechanism whereby RB1 loss causes cell cycle exit in MCF10A cells. During S-phase entry, sustained RAF-MEK-ERK signaling is needed to uphold cyclin D1 expression and repress cyclin inhibitors.[16] In addition, the PI3K-AKT-mTOR signaling cascade facilitates the preservation of cyclin D1 levels by stimulating its translation and impeding its degradation through GSK3β phosphorylation.[17,18] We assessed the phosphorylation profile of these two pathways in RB1-depleted cells. The phosphorylation levels of RAF, MEK1/2, and ERK1/2 were decreased in RB1-depleted MCF10A cells, while diminished MAPK phosphorylation was similarly noted in HMEC but not in MOSE (Figures 2A and S8A,B).

c-Myc is one of the critical ERK substrates in the cell cycle progression. The phosphorylation of c-Myc at serine 62 (pS62) by ERK enhances its stability. Meanwhile, phosphorylation of c-Myc at threonine 58 (pT52) by GSK3β leads to dephosphorylation of Ser62 by protein phosphatase 2A-B56α (PP2AB56α), further causing proteasomal degradation following ubiquitination by SCF-Fbw7 E3 ligase. Consistent with the decrease in the MAPK phosphorylation level, we observed a significant reduction of c-Myc expression in RB1-deficient mammary cells (Figures 2B and S8A). We discovered that pS62 and pT58 of c-Myc were considerably decreased in RB1-deficient cells (Figure 2B), while the mRNA level of c-Myc was unaffected by RB1 loss (Figure S9). Moreover, MG-132, a proteasome inhibitor, restored c-Myc expression in a dose-dependent manner (Figure 2C,D).

Previous report demonstrated that Myc induces altered glutamine metabolism leading to ATP depletion and activation of AMP-activated protein kinase (AMPK) through phosphorylation, ultimately stabilizing p53 protein.[19] In quiescent cells, pyruvate dehydrogenase complex (PDH) activation involves the downregulation of pyruvate dehydrogenase kinases (PDKs). Simultaneously, upregulation of pyruvate dehydrogenase phosphatases (PDPs) occurs, resulting in increased tricarboxylic acid (TCA) cycle activity.[20] To investigate the effect of c-Myc downregulation on cellular metabolism, we confirmed the status of metabolic enzymes in RB1-depleted MCF10A cells. Myc plays a pivotal role in promoting anabolic metabolism which is primarily driven by the degradation of glucose and glutamine.[21,22] In contrast, downregulation of Myc leads to an increase in oxidative phosphorylation through the PDHK1-PDH pathway. AMPK functions as an inhibitory regulator of glycolysis, which consequently accelerates Myc-driven tumorigenesis.[23,24] RB1 loss in MCF10A cells decreased phosphorylation of AMPK and PDH. PDHK1 was found to be downregulated consistent with its function to activate PDH (Figure S10). Our data suggest that the loss of RB1 in mammary epithelial cells results in a reduction of c-Myc

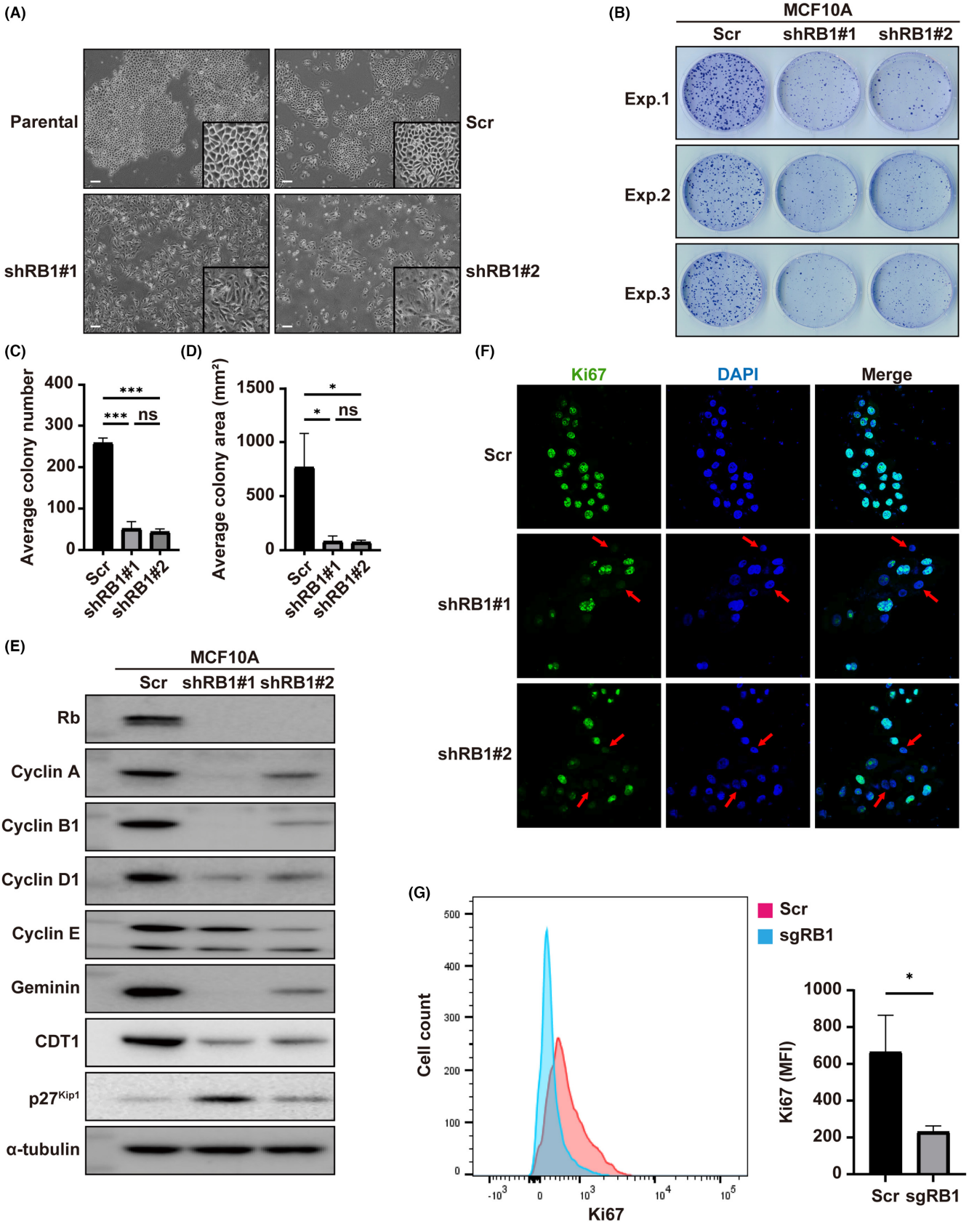


FIGURE 1 Retinoblastoma 1 (RB1) loss induces MCF10A cells' growth arrest. (A) Phase contrast image of MCF10A cells at 72 h after transduction. Scale bar: 200 μm. (B) Representative image of colony formation assay for Scr, shRB1#1, or shRB1#2 in MCF10A. (C) Quantitative analysis of colony number ($N = 3$). (D) Quantitative analysis of colony area ($N = 3$). (E) Immunoblotting of indicated proteins in Scr, shRB1#1, and shRB1#2 MCF10A cells. (F) Immunocytochemistry of Ki67 in MCF10A cells at 72 h after transduction. (G) Immunofluorescence staining of Ki67 in MCF10A cells and quantitative analysis of Ki67 mean fluorescence intensity (MFI) ($N = 3$). *$p < 0.05$, ***$p < 0.001$.

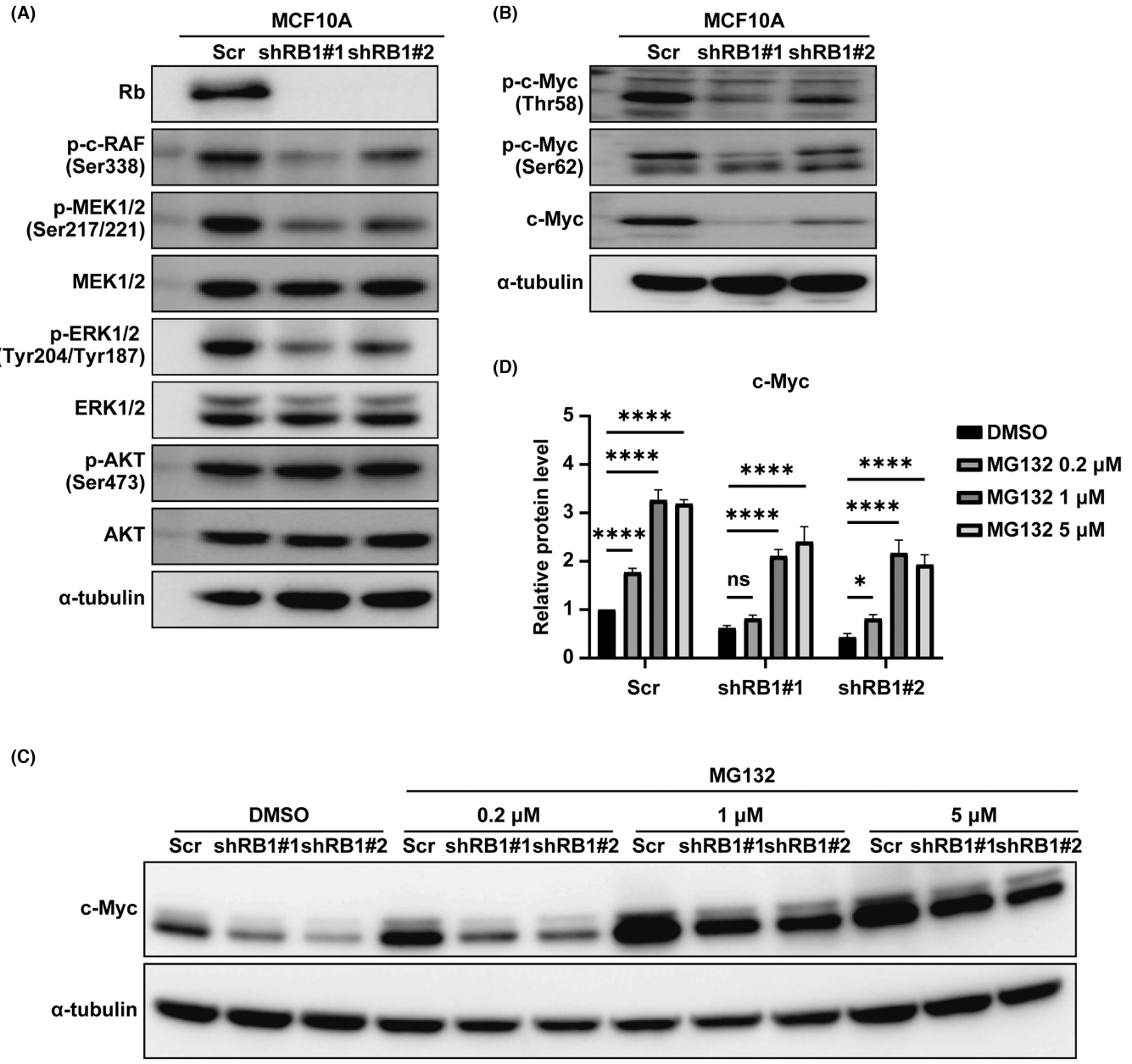


**FIGURE 2** Retinoblastoma 1 (RB1) deletion induces c-Myc downregulation. (A) Immunoblotting of indicated proteins in Scr, shRB1#1, and shRB1#2 MCF10A cells. (B) Immunoblotting of total c-Myc, phospho-c-Myc (Serine 62), and phospho-c-Myc (threonine 58) proteins. (C) Immunoblotting of indicated proteins in Scr, shRB1#1, and shRB1#2 MCF10A cells treated with vehicle or proteasomal inhibitor MG-132. Cells were treated with vehicle or MG132 for 5 h. (D) Quantitative analysis of c-Myc relative protein level ($N = 3$). *$p < 0.05$, ****$p < 0.0001$.

expression through alteration of MAPK activity and is concomitantly linked to metabolic remodeling.

### 3.3 | c-Myc overexpression overrides growth suppression

To further confirm that RB1 loss triggers cell cycle exit in MCF10A cells through c-Myc degradation, we established MCF10A cells in which c-Myc is overexpressed in a DOX-inducible manner. Subsequently, we treated the cells with 1 μg/mL DOX for c-Myc induction, lentivirus for RB1 knockdown, and then puromycin for selection in a sequential manner. After selection, we conducted a colony formation assay. DOX-induced c-Myc overexpression increased the number of colonies in RB-depleted cells, but not in the DOX (–) control (Figure 3A–C). In addition, we assessed the expression of cyclins by Western blotting and found that c-Myc overexpression alleviated their reduced expression in RB1-depleted MCF10A cells. Furthermore, the level of phosphorylated RAF protein was restored in c-Myc overexpressing cells, indicating a recovery of MAPK pathway activity. We also evaluated the expression of chromatin licensing and DNA replication factor 1 (CDT1) in cells overexpressing

c-Myc. Cells with concurrent RB1 depletion and c-Myc overexpression increased CDT1 expression (Figure 3D). Moreover, c-Myc overexpression recovered AMPK phosphorylation level in RB1-deficient cells (Figure S11). Collectively, our data suggest that RB1 depletion-induced cell cycle exit occurs via c-Myc destabilization.

### 3.4 | Overexpression of active RAS restores c-Myc levels and induces transformation

Loss of RB1 activates RAS via upregulation of isoprenylation-related genes through the E2F pathway.[3] Conversely, active RAS increases cyclin D expression and shortens the G1 phase through RB1 phosphorylation. As we observed downregulation of the ERK pathway following RB1 depletion in MCF10A cells (Figure 2A), we examined whether RAS activity was altered in RB1-depleted cells. To measure RAS activity, we performed a RAS-GTP binding assay. We used a RAS-mutant pancreatic cancer cell line MIA-PACA-2 ($KRAS^{G12C}$) as a positive control (Figure S12). GTP-loaded RAS was bound to the RBD of RAF fused to glutathione-S-transferase. Then the $RAS^{GTP}$-RBD complex was captured using glutathione-conjugated beads. RAS activity was quantified by immunoblotting of RAS after pull-down. The activity of N-RAS but not K-RAS was downregulated in RB1 knockdown cells (Figure 4A,B). The RB1-related protein RBL2/p130 participates in the formation of the DREAM (dimerization partner, RB-like, E2F, and multi-vulval class B) complex, thereby contributing to the repression of cell cycle-related genes during quiescence.[25] RBL2/p130 expression was observed to be elevated in RB1-knockout MCF10A cells, whereas RBL1/p107 levels were unaffected (Figure 4C). In contrast, the depletion of RBL2/p130

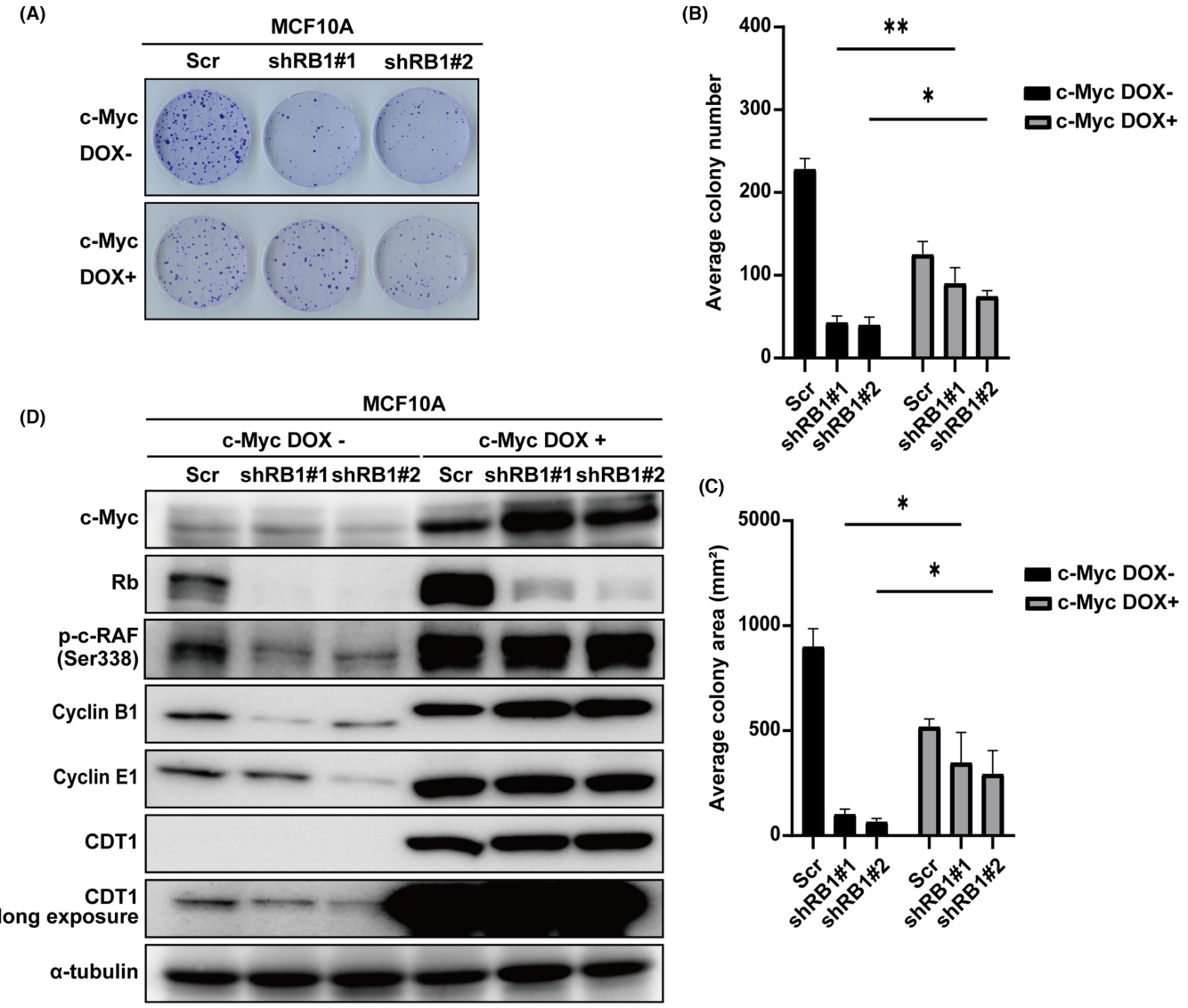


FIGURE 3 c-Myc overexpression overcomes cell growth arrest. (A) Representative image of colony formation assay for MCF10A cells. c-Myc was induced by 1 μg/mL Dox for 72 h in MCF10A. Then, cells were transduced with RBsh lentivirus and subjected to selection by puromycin ($N = 3$). (B) Quantitative analysis of colony number ($N = 3$). (C) Quantitative analysis of colony area ($N = 3$). (D) Immunoblotting of indicated proteins in MCF10A cells. *$p < 0.05$, **$p < 0.01$.

resulted in diminished RB phosphorylation, reduced RAS activity, and the downregulation of farnesyltransferase β (FTβ) (Figure 4D). The reduction of FTβ expression is observed in cells lacking RB1.[3] Furthermore, the simultaneous loss of RB1 and RBL2/p130 led to increased RAS activity and upregulated expression of both c-Myc and FTβ in MCF10A cells.

To investigate whether RAS induces cell cycle progression from quiescence to mitosis, we utilized the DOX induction system to overexpress oncogenically mutated H-RAS$^{G12V}$in RB1-deficient cells. In RB1-negative cells, phospho-c-RAF and phospho-MEK were recovered following H-RAS$^{G12V}$ overexpression. In addition, overexpressed H-RAS$^{G12V}$ recovered c-Myc protein levels. Most importantly, overexpressed H-RAS$^{G12V}$ significantly downregulated p27 levels in MCF10A cells (Figure 4E). As previously reported, oncogenically mutated H-RAS$^{G12V}$ transforms MCF10A and induces colony formation.[26] RB1-intact cells barely formed spheres in the absence of DOX, whereas a significantly increased number of spheres was formed in cells overexpressing oncogenically mutated H-RAS$^{G12V}$ (Figure 4F,G). Notably, upon H-RAS$^{G12V}$ overexpression, RB1-depleted cells exhibited a greater number of spheres than RB-intact cells. These data suggest that the attenuation of RAS activity is a consequence of RBL2/p130 induction, which acts as a counteractive factor , leading to quiescence to impede cellular transformation.

## 4 | DISCUSSION

In this study, we addressed the biological role of RB1 in breast cancer initiation by characterizing RB1-depleted MCF10A cells. We observed that RB1-depleted cells showed β-catenin diffusion, which is one of the phenotypes representing EMT.[27] We examined the expression of EMT markers by immunoblotting and RT-qPCR and found no induction of EMT markers in MCF10A cells following RB1 depletion, although it has been reported that the RB family suppresses ZEB1 expression in p53-intact cells.[28] RB1 depletion induces EMT-like phenotypic and molecular changes in p14$^{ARF}$-deficient MCF7 cells, whereas RB1 overexpression abolishes the EMT-like phenotype in MCF10A cells induced by TGFβ.[29] The tumor suppressor p14$^{ARF}$ is considered a p53 activator and stabilizes and stimulates p53 activity by inhibiting MDM2 and ARF-BP1.[30] p53 regulates EMT through miRNA-200c and miR-183 in nontumorigenic epithelial and tumor cells.[31,32] Moreover, in the absence of the RB family members, oncogenic RAS signaling stabilizes ZEB1 mRNA by suppressing mir-200c.[33] p53 and p14$^{ARF}$ are intact in MCF10A cells, but p14$^{ARF}$ is absent in MCF7 cancer cells. Despite the involvement of a miR-200-mediated interplay between p53 and RB1 and their direct regulation of ZEB1, RB1 depletion alone is insufficient to induce EMT in cells with intact p53. In triple-negative breast cancers (TNBCs), the RB1 loss signature was found to be associated with high β-catenin signaling.[34] The loss of RB1 in TNBC resulted in the upregulation of Wnt-related genes, such as WNT3, FZD9, and LRP8, while the downregulation of Axin2.[34] Notably, the ENCODE ChIP sequencing dataset showed E2F1 binding to the promoter region of LRP8. It might be plausible to hypothesize that the loss of RB1 may activate the β-catenin pathway in the context of mammary epithelium.

In our previous study, RB1 deficiency enhances N-RAS activity, leading to DNA damage-based cellular senescence in calcitonin-positive adenoma.[3] Rb$^{-/-}$; N-ras$^{-/-}$ MEFs bypassed cellular senescence and were able to be transformed by N-RAS$^{G12V}$, while we found that RB1-depleted MCF10A cells exhibiting low RAS activity were transformed by H-RAS$^{G12V}$. RB1-depleted cells can be transformed by oncogenic RAS once they evade the senescence program. While RB1 suppresses components of the replication machinery during cellular senescence, RB1 loss elicits p53/p21$^{WAF/CIP}$-dependent checkpoint preventing escape from cellular senescence.[4] In MCF10A cells, we did not observe the upregulation of DNA damage response-related genes, including p21$^{WAF/CIP}$ following RB1 depletion. MCF10A cells require facilitates chromatin transcription (FACT) to overcome replication stress and cell cycle arrest.[35] RB1 loss-induced replication stress may be buffered by FACT-dependent response, or RB1-deficient cells may enter a quiescent state to reduce DNA replication stress, thereby evading senescence.

In general, the RB1-E2F complex acts as a guardian that prevents excessive cell proliferation, and RB1 deletion leads to uncontrolled cell growth. However, we found that RB1 depletion strongly suppressed MCF10A cell proliferation. The loss of RB1 triggers genome-wide demethylation of histone H3K4, a hallmark of active transcription. This occurs as the binding partner, KDM5A/JARID1A/RBP2, is released from RB1.[36] A histone demethylase, KDM5A, was originally identified by screening proteins that bind to pRB mutants but are incapable of binding to E2Fs. The ENCODE ChIP sequencing dataset revealed that KDM5A could bind to the promoter region of FTβ, and EGFR.[37] We observed a reduction of EGFR expression and phosphorylation in RB1-knockout MCF10A cells (Figure 4C). The genomic region on chromosome 12p that encodes for KDM5A is frequently amplified in patients with breast cancer. Furthermore, the inhibition of KDM5A expression has been shown to sensitize breast cancer cells to EGFR inhibitors.[38] Therefore, KDM5A activated by

**FIGURE 4** Overexpression of active RAS restores c-Myc levels and induces transformation. (A) Pull-down assay of RAS protein and GTP protein. Pan-RAS protein was analyzed by immunoblotting. α-tubulin was used as a loading control. (B) Quantitative analysis of RAS activity (RAS-GTP/Pan-RAS, $N=3$). (C) Immunoblotting of indicated proteins in MCF10A cells using CRISPR. (D) Immunoblotting of indicated protein in MCF10A cells after induction of gRNA for retinoblastoma 1 (RB1) and RBL2. (E) Immunoblotting of indicated proteins in MCF10A cells. Cells were transduced with lentivirus harboring tetracycline-inducible mutant RAS and subjected to selection with 200 μg/mL hygromycin under DOX (–) condition. Then, cells were transduced with RBsh lentivirus and subjected to selection with puromycin. After selection, cells were treated with 1 μg/mL doxycycline for 24 h and analyzed by immunoblotting. (F) Phase contrast image of MCF10A cells in sphere assay. Scale bar: 200 μm. (G) Quantitative analysis of sphere number (sphere size >25,000 μm$^2$, $N=3$). *$p<0.05$, ***$p<0.001$, ****$p<0.0001$.

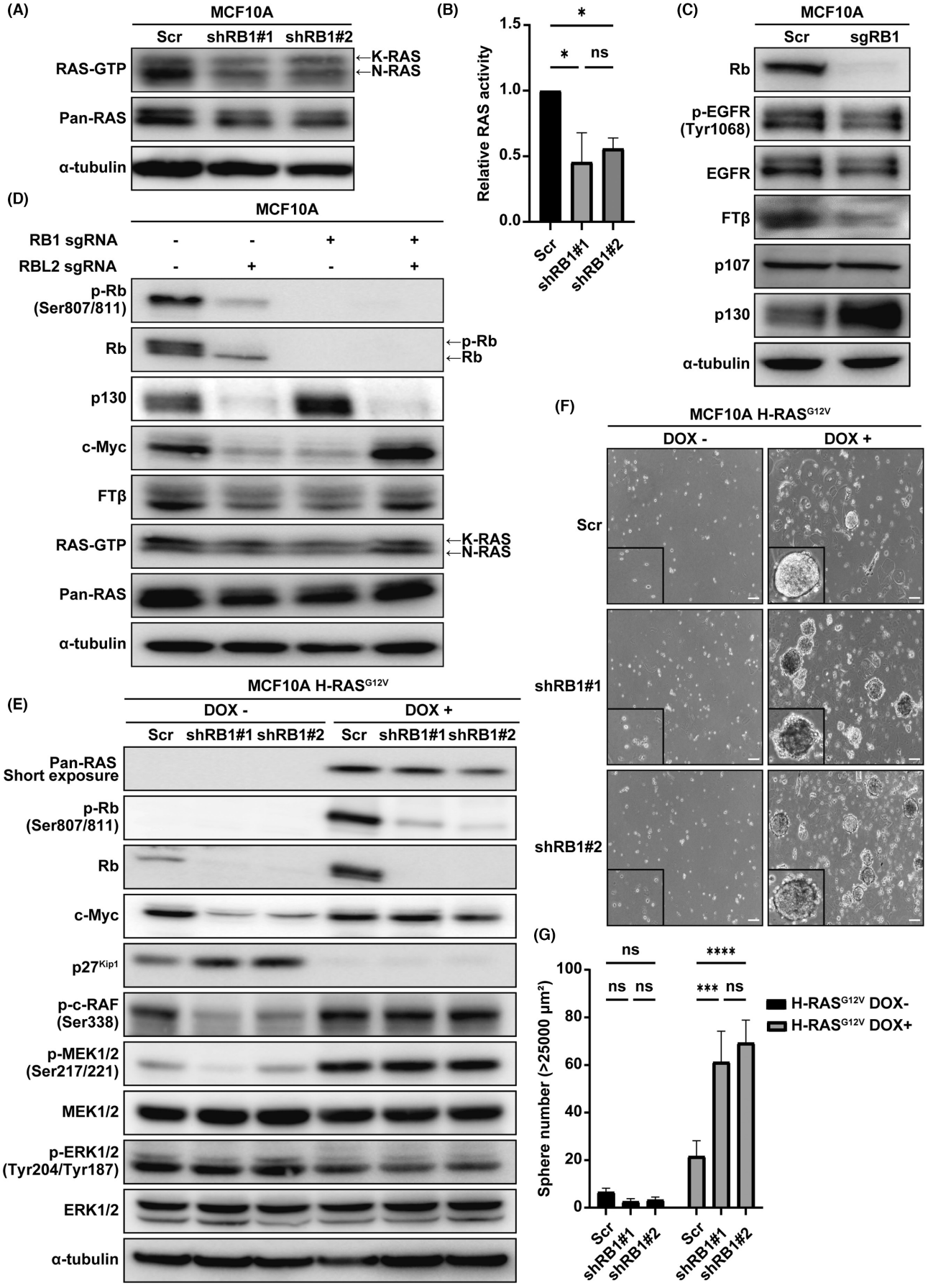
(A)
MCF10A
Scr
shRB1#1
shRB1#2
RAS-GTP
←K-RAS
←N-RAS
Pan-RAS
α-tubulin
(B)
Relative RAS activity
1.5
1.0
0.5
0.0
*
* ns
Scr
shRB1#1
shRB1#2
(C)
MCF10A
Scr
sgRB1
Rb
p-EGFR (Tyr1068)
EGFR
FTβ
p107
p130
α-tubulin
(D)
MCF10A
RB1 sgRNA - - + +
RBL2 sgRNA - + - +
p-Rb (Ser807/811)
Rb
←p-Rb
←Rb
p130
c-Myc
FTβ
RAS-GTP
←K-RAS
←N-RAS
Pan-RAS
α-tubulin
(E)
MCF10A H-RAS$^{G12V}$
DOX - DOX +
Scr shRB1#1 shRB1#2 Scr shRB1#1 shRB1#2
Pan-RAS Short exposure
p-Rb (Ser807/811)
Rb
c-Myc
p27$^{Kip1}$
p-c-RAF (Ser338)
p-MEK1/2 (Ser217/221)
MEK1/2
p-ERK1/2 (Tyr204/Tyr187)
ERK1/2
α-tubulin
(F)
MCF10A H-RAS$^{G12V}$
DOX - DOX +
Scr
shRB1#1
shRB1#2
(G)
Sphere number (>25000 μm²)
100
80
60
40
20
0
ns
ns ns
****
*** ns
H-RAS$^{G12V}$ DOX-
H-RAS$^{G12V}$ DOX+
Scr
shRB1#1
shRB1#2
Scr
shRB1#1
shRB1#2

RB loss may suppress the expression of EGFR, which is upstream of RAS-MEK-ERK. Moreover, FTβ-mediated isoprenylation is essential for RAS maturation and exhibits reduced expression in cells lacking RB1. KDM5A may act as a functional equivalent to compensate for spontaneous RB loss, thus impeding abnormal proliferation of normal epithelial cells.

## AUTHOR CONTRIBUTIONS

**Linxiang Gong:** Data curation; formal analysis; investigation; writing – original draft. **Dominic Voon:** Supervision; writing – review and editing. **Joji Nakayama:** Writing – review and editing. **Chiaki Takahashi:** Conceptualization; funding acquisition; project administration; supervision; writing – review and editing. **Susumu Kohno:** Conceptualization; funding acquisition; methodology; project administration; resources; supervision; writing – original draft.

## ACKNOWLEDGMENTS

We are grateful to Y. Johmura for generously providing the H-RAS$^{G12V}$ construct. We thank members of the Takahashi Laboratory for their helpful suggestions and proofreading.

## FUNDING INFORMATION

This study was supported by Grant-in-Aid for Scientific Research (17K14992 and 20K07612 to SK; 22K07209 to DV; and 17H03576, 17K19586, and 19K22555 to CT) and Grant-in-Aid for JSPS Fellows (23KJ1033 to LG) from MEXT; Funding Program for Next Generation World-Leading Researchers (LS049) from the Cabinet Office of Japan; Project for Cancer Research and Therapeutic (P-CREATE) (19cm0106164h0001) from the Japan Agency for Medical Research and Development (AMED); and TaNeDS (C1010568) from Daiichi-Sankyo.

## CONFLICT OF INTEREST STATEMENT

The authors have no financial interest to disclose. Dr. Chiaki Takahashi is an associate editor of *Cancer Science*.

## ETHICS STATEMENT

Approval of the research protocol by an Institutional Reviewer Board: N/A.

Informed Consent: N/A.

Registry and the Registration No. of the study/trial: N/A.

Animal Studies: N/A.

## ORCID

*Dominic Chih-Cheng Voon* https://orcid.org/0000-0002-2963-9305

*Chiaki Takahashi* https://orcid.org/0000-0003-3390-9563

*Susumu Kohno* https://orcid.org/0000-0002-1448-9527

## REFERENCES

1. Witkiewicz AK, Knudsen ES. Retinoblastoma tumor suppressor pathway in breast cancer: prognosis, precision medicine, and therapeutic interventions. *Breast Cancer Res*. 2014;16:207.
2. Knudsen ES, Nambiar R, Rosario SR, Smiraglia DJ, Goodrich DW, Witkiewicz AK. Pan-cancer molecular analysis of the RB tumor suppressor pathway. *Commun Biol*. 2020;3:158.
3. Shamma A, Takegami Y, Miki T, et al. Rb regulates DNA damage response and cellular senescence through E2F-dependent suppression of N-ras isoprenylation. *Cancer Cell*. 2009;15:255-269.
4. Chicas A, Wang X, Zhang C, et al. Dissecting the unique role of the retinoblastoma tumor suppressor during cellular senescence. *Cancer Cell*. 2010;17:376-387.
5. Marescal O, Cheeseman IM. Cellular mechanisms and regulation of quiescence. *Dev Cell*. 2020;55:259-271.
6. Besson A, Gurian-West M, Chen X, Kelly-Spratt KS, Kemp CJ, Roberts JM. A pathway in quiescent cells that controls p27Kip1 stability, subcellular localization, and tumor suppression. *Genes Dev*. 2006;20:47-64.
7. Sheng J, Kohno S, Okada N, et al. Treatment of retinoblastoma 1-intact hepatocellular carcinoma with cyclin-dependent kinase 4/6 inhibitor combination therapy. *Hepatology*. 2021;74:1971-1993.
8. Guiley KZ, Stevenson JW, Lou K, et al. p27 allosterically activates cyclin-dependent kinase 4 and antagonizes palbociclib inhibition. *Science*. 2019;366:eaaw2106.
9. Kitajima S, Yoshida A, Kohno S, et al. The RB-IL-6 axis controls self-renewal and endocrine therapy resistance by fine-tuning mitochondrial activity. *Oncogene*. 2017;36:5145-5157.
10. Zavadil J, Böttinger EP. TGF-beta and epithelial-to-mesenchymal transitions. *Oncogene*. 2005;24:5764-5774.
11. Brown KA, Aakre ME, Gorska AE, et al. Induction by transforming growth factor-beta1 of epithelial to mesenchymal transition is a rare event in vitro. *Breast Cancer Res*. 2004;6:R215-R231.
12. Schuhwerk H, Kleemann J, Gupta P, et al. The EMT transcription factor ZEB1 governs a fitness-promoting but vulnerable DNA replication stress response. *Cell Rep*. 2022;41:111819.
13. Jönsson G, Staaf J, Olsson E, et al. High-resolution genomic profiles of breast cancer cell lines assessed by tiling BAC array comparative genomic hybridization. *Genes Chromosomes Cancer*. 2007;46:543-558.
14. Abbas T, Dutta A. p21 in cancer: intricate networks and multiple activities. *Nat Rev Cancer*. 2009;9:400-414.
15. Duronio RJ, Xiong Y. Signaling pathways that control cell proliferation. *Cold Spring Harb Perspect Biol*. 2013;5:a008904.
16. Lavoie H, Gagnon J, Therrien M. ERK signalling: a master regulator of cell behaviour, life and fate. *Nat Rev Mol Cell Biol*. 2020;21:607-632.
17. Alao JP. The regulation of cyclin D1 degradation: roles in cancer development and the potential for therapeutic invention. *Mol Cancer*. 2007;6:24.
18. Nicholson KM, Anderson NG. The protein kinase B/Akt signalling pathway in human malignancy. *Cell Signal*. 2002;14:381-395.
19. Nieminen AI, Eskelinen VM, Haikala HM, et al. Myc-induced AMPK-phospho p53 pathway activates Bak to sensitize mitochondrial apoptosis. *Proc Natl Acad Sci USA*. 2013;110:E1839-E1848.
20. Salama R, Sadaie M, Hoare M, Narita M. Cellular senescence and its effector programs. *Genes Dev*. 2014;28:99-114.
21. Stine ZE, Walton ZE, Altman BJ, Hsieh AL, Dang CV. MYC, metabolism, and cancer. *Cancer Discov*. 2015;5:1024-1039.
22. Wise DR, DeBerardinis RJ, Mancuso A, et al. Myc regulates a transcriptional program that stimulates mitochondrial glutaminolysis and leads to glutamine addiction. *Proc Natl Acad Sci USA*. 2008;105:18782-18787.
23. Faubert B, Boily G, Izreig S, et al. AMPK is a negative regulator of the Warburg effect and suppresses tumor growth in vivo. *Cell Metab*. 2013;17:113-124.
24. Tong WH, Sourbier C, Kovtunovych G, et al. The glycolytic shift in fumarate-hydratase-deficient kidney cancer lowers AMPK levels, increases anabolic propensities and lowers cellular iron levels. *Cancer Cell*. 2011;20:315-327.

25. Litovchick L, Sadasivam S, Florens L, et al. Evolutionarily conserved multisubunit RBL2/p130 and E2F4 protein complex represses human cell cycle-dependent genes in quiescence. *Mol Cell*. 2007;26:539-551.
26. Ciardiello F, McGeady ML, Kim N, et al. Transforming growth factor-alpha expression is enhanced in human mammary epithelial cells transformed by an activated c-ha-ras protooncogene but not by the c-neu protooncogene, and overexpression of the transforming growth factor-alpha complementary DNA leads to transformation. *Cell Growth Differ*. 1990;1:407-420.
27. Morali OG, Delmas V, Moore R, Jeanney C, Thiery JP, Larue L. IGF-II induces rapid beta-catenin relocation to the nucleus during epithelium to mesenchyme transition. *Oncogene*. 2001;20:4942-4950.
28. Liu Y, Sánchez-Tilló E, Lu X, et al. The ZEB1 transcription factor acts in a negative feedback loop with miR200 downstream of Ras and Rb1 to regulate Bmi1 expression. *J Biol Chem*. 2014;289:4116-4125.
29. Arima Y, Inoue Y, Shibata T, et al. Rb depletion results in deregulation of E-cadherin and induction of cellular phenotypic changes that are characteristic of the epithelial-to-mesenchymal transition. *Cancer Res*. 2008;68:5104-5112.
30. Bieging KT, Mello SS, Attardi LD. Unravelling mechanisms of p53-mediated tumour suppression. *Nat Rev Cancer*. 2014;14:359-370.
31. Chang CJ, Chao CH, Xia W, et al. p53 regulates epithelial-mesenchymal transition and stem cell properties through modulating miRNAs. *Nat Cell Biol*. 2011;13:317-323.
32. Dong P, Karaayvaz M, Jia N, et al. Mutant p53 gain-of-function induces epithelial-mesenchymal transition through modulation of the miR-130b-ZEB1 axis. *Oncogene*. 2013;32:3286-3295.
33. Liu Y, Sánchez-Tilló E, Lu X, et al. Sequential inductions of the ZEB1 transcription factor caused by mutation of Rb and then Ras proteins are required for tumor initiation and progression. *J Biol Chem*. 2013;288:11572-11580.
34. Wang DY, Gendoo DMA, Ben-David Y, Woodgett JR, Zacksenhaus E. A subgroup of microRNAs defines PTEN-deficient, triple-negative breast cancer patients with poorest prognosis and alterations in RB1, MYC, and Wnt signaling. *Breast Cancer Res*. 2019;21:18.
35. Prendergast L, Hong E, Safina A, Poe D, Gurova K. Histone chaperone FACT is essential to overcome replication stress in mammalian cells. *Oncogene*. 2020;39:5124-5137.
36. Chicas A, Kapoor A, Wang X, et al. H3K4 demethylation by Jarid1a and Jarid1b contributes to retinoblastoma-mediated gene silencing during cellular senescence. *Proc Natl Acad Sci USA*. 2012;109:8971-8976.
37. Consortium EP. The ENCODE (ENCyclopedia of DNA elements) project. *Science*. 2004;306:636-640.
38. Hou J, Wu J, Dombkowski A, et al. Genomic amplification and a role in drug-resistance for the KDM5A histone demethylase in breast cancer. *Am J Transl Res*. 2012;4:247-256.

## SUPPORTING INFORMATION

Additional supporting information can be found online in the Supporting Information section at the end of this article.

**How to cite this article:** Gong L, Voon D-C, Nakayama J, Takahashi C, Kohno S. RB1 loss induces quiescent state through downregulation of RAS signaling in mammary epithelial cells. *Cancer Sci*. 2024;115:1576-1586. doi:10.1111/cas.16122